The stable strontium isotopic composition of ocean island basalts, mid-ocean ridge basalts, and komatiites

Elsa Amsellem, Frédéric Moynier, James M.D. Day, Manuel Moreira, Igor Puchtel, Fang-Zhen Teng

To cite this version:

Elsa Amsellem, Frédéric Moynier, James M.D. Day, Manuel Moreira, Igor Puchtel, et al.. The stable strontium isotopic composition of ocean island basalts, mid-ocean ridge basalts, and komatiites. Chemical Geology, 2018, 483, pp.595-602. 10.1016/j.chemgeo.2018.03.030 . insu-02917170

HAL Id: insu-02917170
https://insu.hal.science/insu-02917170

Chemical Geology 483 (2018) 595–602

Contents lists available at ScienceDirect

Chemical Geology

journal homepage: www.elsevier.com/locate/chemgeo

The stable strontium isotopic composition of ocean island basalts, mid-ocean ridge basalts, and komatiites

Elsa Amsellem[a,⁎], Frédéric Moynier[a,b], James M.D. Day[a,c], Manuel Moreira[a], Igor S. Puchtel[d], Fang-Zhen Teng[e]

[a] *Institut de Physique du Globe de Paris, Université Paris Diderot, Sorbonne Paris Cité, CNRS UMR 7154, 1 rue Jussieu, 75238 Paris, France*
[b] *Institut Universitaire de France, Paris, France*
[c] *Scripps Institution of Oceanography, University of California San Diego, La Jolla, CA 92093-0244, USA*
[d] *Department of Geology, University of Maryland, 237 Regents Drive, College Park, MD 20742, USA*
[e] *Department of Earth and Space Sciences, University of Washington, Seattle, WA 98195-1310, USA*

ARTICLE INFO

Keywords:
Sr isotopes
Ocean island basalts
Mid-ocean ridge basalts
Komatiites
Kilauea Iki
Bulk silicate earth

ABSTRACT

The radiogenic ^{87}Rb-^{87}Sr system has been widely applied to the study of geological and planetary processes. In contrast, the stable Sr isotopic composition of the bulk silicate Earth (BSE) and the effects of igneous differentiation on stable Sr isotopes are not well-established. Here we report the stable Sr isotope (^{88}Sr/^{86}Sr, reported as $\delta^{88/86}$Sr, in parts per mil relative to NIST SRM 987) compositions for ocean islands basalts (OIB), mid-ocean ridge basalts (MORB) and komatiites from a variety of locations. Stable Sr isotopes display limited fractionation in a OIB sample suite from the Kilauea Iki lava lake suggesting that igneous processes have limited effect on stable Sr isotope fractionation ($\pm$0.12‰ over 20% MgO variation; 2sd). In addition, OIB ($\delta^{88/86}$Sr = 0.16–0.46‰; average 0.28 ± 0.17‰), MORB ($\delta^{88/86}$Sr = 0.27–0.34‰; average 0.31 ± 0.05‰) and komatiites ($\delta^{88/86}$Sr = 0.20–0.97‰; average 0.41 ± 0.16‰) from global localities exhibit broadly similar Sr stable isotopic compositions. Heavy stable Sr isotope compositions ($\delta^{88/86}$Sr > 0.5‰) in some Barberton Greenstone belt komatiites may reflect Archean seawater alteration or metamorphic processes and preferential removal of the lighter isotopes of Sr. To first order, the similarity among OIBs from three different ocean basins suggests homogeneity of stable Sr isotopes in the mantle. Earth's mantle stable Sr isotopic composition is established from the data on OIB, MORB and komatiites to be $\delta^{88/86}$Sr = 0.30 ± 0.02‰ (2sd). The BSE $\delta^{88/86}$Sr value is identical, within uncertainties, to the composition of carbonaceous chondrites ($\delta^{88/86}$Sr = 0.29 ± 0.06‰; 2sd) measured in this study.

1. Introduction

Strontium is an alkaline earth metal and refractory lithophile element, with a 50% condensation temperature (Tc) of 1464 K (Lodders, 2003). It has three stable isotopes - ^{84}Sr (0.56%), ^{86}Sr (9.86%), ^{88}Sr (82.58%) – and a long-lived radiogenic isotope, ^{87}Sr (7.00%), a daughter product of ^{87}Rb ($T_{1/2} = 49.75 \times 10^9$ years, Nebel et al., 2011). Due to differences in volatility and partitioning behaviour during igneous processes of Rb and Sr, the ^{87}Rb-^{87}Sr system has seen wide application as a chronometer and tracer in geochemistry and cosmochemistry (e.g., Papanastassiou and Wasserburg, 1969; Birck and Allègre, 1973). In general, for Rb-Sr isotope chronology, the ^{88}Sr/^{86}Sr ratio is used as a normalization ratio to correct for instrumental mass-dependent effects using either thermal-ionization (TIMS) or multi-collector inductively-coupled-plasma (MC-ICP-MS) mass-spectrometry.

Utilizing non-traditional stable isotopes to understand a range of geological processes (e.g., Teng et al., 2017) has led to proliferation of high-precision stable isotopic measurements of Sr by either double-spike methods using TIMS (e.g., Parkinson et al., 2007; Pearce et al., 2015; Stevenson et al., 2014; Charlier et al., 2017) or MC-ICP-MS (e.g., Shalev et al., 2013), or by sample-standard bracketing with MC-ICP-MS (e.g., Halicz et al., 2008; Moynier et al., 2010; De Souza et al., 2010). Such studies have shown that biogenic and inorganic Ca-carbonates tend to be enriched in the lighter isotopes of Sr, while seawater is enriched in the heavier isotopes compared to the NIST SRM987 standard, which is a highly purified and homogenized Sr carbonate (Ohno and Hirata, 2007; Krabbenhöft et al., 2010; Raddatz et al., 2013). Stable isotopes of Sr are also used as tracers of continental weathering (e.g., Wei et al., 2013; Stevenson et al., 2016), and are proxies for paleotemperature (Stevenson et al., 2014; Fietzke and Eisenhauer, 2006;

⁎ Corresponding author.
E-mail address: amsellem@ipgp.fr (E. Amsellem).

https://doi.org/10.1016/j.chemgeo.2018.03.030
Received 9 November 2017; Received in revised form 16 March 2018; Accepted 17 March 2018

Vollstaedt et al., 2014).

Studies of extra-terrestrial materials have found that chondrules and calcium aluminium-rich inclusions (CAIs) of the carbonaceous chondrite Allende are enriched in the lighter isotopes of Sr relative to the bulk rock, while terrestrial and extra-terrestrial materials have similar $^{88}Sr/^{86}Sr$ ratios within ~50 ppm (Patchett, 1980; Moynier et al., 2010; Charlier et al., 2012). Moynier et al. (2010) proposed that the isotopically light CAIs (down to ~ − 1.7‰ for $^{88}Sr/^{86}Sr$ ratios compared to bulk meteorites) resulted from electromagnetic sorting of ionized heavy Sr from neutral Sr in the early Solar System, while Patchett (1980) suggested that CAIs were isotopically fractionated during volatilization processes.

Given the applications described above, advancing our knowledge of Sr isotopic variability in terrestrial igneous rocks is fundamental for two principle reasons. First, the interpretation of Sr isotope applied to understand weathering processes relies on the fact that the high-temperature fractionation of Sr isotopes is well-understood and that isotopic variations in weathering products do not reflect this important process. Second, the extent of Sr isotopic fractionation during igneous processes, as well as the estimation of the isotopic composition of the Earth's mantle and of the bulk silicate Earth (BSE), are central to any inter-planetary comparisons. However, the isotopic composition of the BSE has only been estimated from a limited number of terrestrial igneous rocks, including < 20 basalts (mostly from Hawaii, including many replicates of BHVO-2), a large set of rhyolites and several granites and andesites (Charlier et al., 2012, 2017, Moynier et al., 2010). While the Sr isotopic composition of the basalts, granites, and andesites cluster around the same value, several rhyolite glasses were reported to be enriched in the lighter Sr isotopes and it was suggested that igneous differentiation may cause Sr isotopic fractionation (Charlier et al., 2012). It is therefore possible that basalts may not be representative of their mantle source due to the effects of igneous fractionation on stable Sr isotopes.

To precisely determine the behavior of Sr isotopes during magmatic differentiation and establish the composition of BSE, it is necessary to investigate natural terrestrial samples from a common source. Kilauea Iki (KI) lava lake is well-suited to test the effects of fractional crystallization because these samples were formed in a closed system and have experienced extensive fractional crystallization, with MgO contents ranging from 26.9 to 2.4 wt% (Helz et al., 1994; 2012). They have therefore been used widely to study stable isotopic fractionation during igneous processes (e.g., Zn: Chen et al., 2013; Ga: Kato et al., 2017; Fe: Teng et al., 2008; Mg: Teng et al., 2010; Sn: Badullovich et al., 2017; Li: Tomascak et al., 1999). To evaluate the Sr isotopic composition of BSE we report data to test the effect of igneous differentiation on a series of Kilauea Iki lava lake samples, and to evaluate the spatial and temporal heterogeneity of Sr stable isotope compositions in the terrestrial mantle using basaltic rocks from different settings (ocean island basalts [OIB], mid ocean ridge basalts [MORB], continental flood basalts [CFB], and komatiites). We also report data for a variety of chondritic meteorites for comparison with the estimated BSE Sr isotopic composition.

2. Materials and methods

2.1. Samples

A set of forty-five basalts were selected for stable Sr isotopic analysis, including thirty-seven OIB, seven MORB from the Pacific, Atlantic and Indian Oceans, and one CFB (BCR-2). One of the MORB samples (EW9309-20D) comes from the Shona ridge anomaly, where there is evidence of plume-ridge interaction (Moreira et al., 1995). For the OIB, we selected samples covering a large range of compositions (Table 1). For example, St. Helena is classified as HIMU-like based on its radiogenic isotopes, and has low $^{3}He/^{4}He$ (Graham et al., 1992; Hanyu and Kaneoka, 1997). Seven samples from the Canary Islands, including the islands of La Palma, El Hierro, Gran Canaria, and Fuerteventura, are considered to contain variable and distinct proportions of recycled oceanic crust and lithosphere as evidenced from He-O-Sr-Nd-Os-Pb isotopes (e.g., Day et al., 2009, 2010; Day and Hilton, 2011). Three samples from volcanic complexes in the Northern Rift Zone in Iceland have depleted tholeiitic compositions. OIB samples from Iceland have attracted many studies because of the association between an oceanic ridge and a mantle plume (Rickers et al., 2013). It has been suggested, based on unradiogenic He and Ne, that the source of these samples is deep, undegassed mantle (Breddam et al., 2000; Moreira et al., 2001). The remaining samples come from several ocean island localities in the Pacific, Indian and Atlantic ocean basins and have been previously characterized for major- and trace-elements, radiogenic isotopes, and Si and Ga stable isotopic compositions (LeRoex, 1985; Albarède and Tamagnan, 1988; Breddam et al., 2000; Claude-Ivanaj et al., 2001; Breddam, 2002; Workman et al., 2004; Geist et al., 2006; Jackson et al., 2007a, 2007b; Millet et al., 2008; Kurz et al., 2009; Day et al., 2010; Kawabata et al., 2011; Hart and Jackson, 2014; Garapić et al., 2015, Pringle et al., 2016, Peters & Day, 2017; Kato et al., 2017).

Samples that we analyzed from the Kilauea Iki lava lake were erupted in 1959 to form a 135 m deep lava lake. Drilling of the lava lake has afforded the opportunity to study the entire igneous sequence preserved during cooling and crystallization (Helz, 2012). The Kilauea Iki lava lake was formed from picritic lava with an average MgO content of ~15.4 wt% (Wright, 1973). The chemical evolution of the lava is controlled mainly by the olivine content with a range from olivine-rich cumulates, through olivine tholeiites, ferro-diabases and andesites (Helz and Thornber, 1987). We selected eight drill core and two surface outcrop samples (Iki-22, Iki-58). The MgO contents of these samples vary from 25.8 to 2.4 wt%, and the SiO_2 content from 44.6 to 57.1 wt% (Helz et al., 1994; Helz, 2012). The Li, Mg, Fe, Zn, Cu and Ga isotopic compositions for these samples have also previously been reported (see Tomascak et al., 1999; Teng et al., 2007, 2008, 2010, 2011, Chen et al., 2013; Savage et al., 2015; Kato et al., 2017).

We analyzed 2.69 Ga komatiites from the Belingwe Greenstone Belt in Zimbabwe (TN17, TN18, TN19, ZV10). These are drill core and surface outcrop samples reported previously by Puchtel et al. (2009) for Pt-Re-Os and Sm-Nd isotopes, and for their HSE (highly siderophile elements) and REE (rare earth elements) abundance systematics. The 2.41 Ga komatiite samples 01001, 01104, 01105 from the Victoria's Lava Lake from the Vetreny Belt, Fennoscandia, are olivine cumulates studied by Greber et al. (2015) for Mo stable isotopic composition, and by Puchtel et al. (2016) for Pt-Re-Os, ^{142}Nd, ^{182}W, and HSE abundance systematics. These komatiites are known to have assimilated ~4% of upper crustal material (Puchtel et al., 2016). Komatiites from the Barberton Greenstone belt in South Africa were analyzed, including 3.48 Ga Komati formation samples (BV03, BV10, BV13, BV15 from the lower to the upper part of the surface outcrop), and a single sample from the 3.27 Ga Weltevreden formation (501-1) previously studied by Puchtel et al. (2013, 2014) and Greber et al. (2015). Since komatiites are produced by high degrees (25–40%) of partial melting (e.g., Herzberg, 1992), and Sr behaves as an incompatible element, komatiite melts quantitatively extract Sr from the mantle sources, which permits assessment of the temporal and spatial Sr isotopic heterogeneity of Earth's mantle and possible fractionation during partial melting between komatiites, OIB and MORB.

Eight chondrite samples were studied for comparison with terrestrial samples. These included six carbonaceous chondrites - Vigarano (CV3), Felix (CO3), Isna (CO3), Cold Bokkeveld (CM2), Jbilet Winselwan (CM2) and Maralinga (CK4), one ordinary chondrite, Krymka (LL3), and one enstatite chondrite, Abee (EH4).

2.2. Sample purification

Between 7 and 100 mg of un-leached sample powder was dissolved in a 3:1 mixture of HF and HNO_3 in Teflon bombs. The bombs were placed on a hot plate for 2 days at 120 °C. The samples were evaporated

Table 1
Stable strontium isotopic composition of terrestrial basalts and komatiites relative to NIST SRM987.

Sample	Location	Ocean	$\delta^{88/86}$Sr	2se[a]	SiO$_2$	MgO	n[b]
Basalts							
BCR-2	Columbia River	–	0.29	0.01	54.1	3.59	10
LP03	La Palma	Atlantic	0.42	0.03	39.04[d]	28.7[c]	5
LP04	La Palma	Atlantic	0.28	0.04		7.9[c]	3
LP15	La Palma	Atlantic	0.22	0.01	43.23[d]		3
FE0903	Fuerteventura	Atlantic	0.27	0.01	47.05[d]		5
FE0904	Fuerteventura	Atlantic	0.23	0.03			5
GC0902	Gran Canaria	Atlantic	0.46	0.02			5
GC0906	Gran Canaria	Atlantic	0.27	0.03			2
EH15	El Hierro	Atlantic	0.26	0.01	42.27[d]	17.6[c]	2
EH07	El Hierro	Atlantic	0.18	0.02		11.7[c]	2
EH12	El Hierro	Atlantic	0.18	0.02	42.08[d]	13.5[c]	2
EH03	El Hierro	Atlantic	0.31	0.01	42.74[d]	12.8[c]	3
CVSN 98-18	Cape Verde	Atlantic	0.25	0.02	44.3[d]		5
CVSN 98-19	Cape Verde	Atlantic	0.25	0.01			5
ACO 95-3 San Miguel	Azores	Atlantic	0.27	0.03	47.81[d]		5
ACO 2000 52	Azores	Atlantic	0.27	0.02			5
SH25	St Helena	Atlantic	0.36	0.05	44.95[d]		5
SH25 (replicate)	St Helena	Atlantic	0.32	0.02	44.95[d]		5
SH25 mean	St Helena	Atlantic	0.34	0.04			
BV2	Bouvet	Atlantic	0.18	0.05	55.16[d]		5
BM 1962, 128 (114)	Tristan da Cunha	Atlantic	0.24	0.03	43.14[d]		5
ALR-40G	Gough	Atlantic	0.16	0.04	48.54[d]		5
KBD 408 730	Iceland	Atlantic	0.30	0.03			2
151 09-9	Iceland	Atlantic	0.33	0.02	44.34[d]		5
SK 82-28	Iceland	Atlantic	0.46	0.02			5
MD50 CP112	St Paul-Amsterdam	Indian	0.22	0.03	43.91[d]		5
ERRUPTION 1931	Reunion	Indian	0.45	0.06			5
RU0713	Reunion	Indian	0.43	0.04	43.3[h]	29.07[h]	5
RU0701	Reunion	Indian	0.25	0.02	42.1[h]	23.5[h]	5
RU0701 (replicate)	Reunion	Indian	0.29	0.005			2
RU0701 mean	Reunion	Indian	0.27	0.04			
AHANEMO2 D20-B	Galapagos	Pacific	0.29	0.03			
Average OIB			0.29	0.03			28
RD87 DR29-101	Mid Atlantic Ridge	Atlantic	0.29	0.01			5
EW9309-20D	Mid Atlantic Ridge	Atlantic	0.27	0.03			5
EW9309-20D (replicate)	Mid Atlantic Ridge	Atlantic	0.28	0.03			5
EW9309-20D mean	Mid Atlantic Ridge	Atlantic	0.27	0.01			
DIVA 1 13-3	Mid Atlantic Ridge	Atlantic	0.32	0.02			4
SWIFT DR32-1	Southwest Indian Ridge	Indian	0.33	0.03			4
MD57 D2-8	Central Indian Ridge	Indian	0.34	0.01			4
SEARISE 2 DR3	East Pacific Ridge	Pacific	0.31	0.04			5
PAC 2 DR38	Pacific Antarctic Ridge	Pacific	0.32	0.03			5
Average MORB			0.31	0.02			7
KI 19-IRI-170.9	Kilauea IKI	Pacific	0.24	0.06	54.59[e]	3.48[e]	3
IKI-58	Kilauea IKI	Pacific	0.28	0.04	49.91[c]	8.08[c]	3
KI-79-150.4	Kilauea IKI	Pacific	0.29	0.02	48.44[e]	13.5[e]	3
KI-81-2-88.6	Kilauea IKI	Pacific	0.42	0.02	57.07[e]	2.37[e]	3
KI-75-1-15.2	Kilauea IKI	Pacific	0.31	0.02	50.13[e]	5.77[e]	3
IKI 22	Kilauea IKI	Pacific	0.36	0.03	46.68[e]	19.52[e]	3
KI 67-3-58.0	Kilauea IKI	Pacific	0.29	0.02	49.64[e]	8.91[e]	3
KI 67-2-85.7	Kilauea IKI	Pacific	0.36	0.04	56.21[e]	2.6[e]	3
KI 67-3-6.8	Kilauea IKI	Pacific	0.20	0.01	44.63[e]	25.83[e]	3
KI 15-1-121.5	Kilauea IKI	Pacific	0.31	0.01	50[e]	7.77[e]	3
Average Kilauea Iki			0.31	0.04			10
Komatiites							
TN17	Belingwe Greenstone Belt		0.44	0.04	44.7[f]	31.3[f]	4
TN18	Belingwe Greenstone Belt		0.20	0.08	45.2[f]	30.4[f]	4
TN19	Belingwe Greenstone Belt		0.35	0.08	45.3[f]	30.3[f]	4
ZV10	Belingwe Greenstone Belt		0.45	0.07	46.2[f]	27.5[f]	2
O1001	Victoria's lava lake (Vetreny Belt)		0.29	0.02			5
O1104	Victoria's lava lake (Vetreny Belt)		0.25	0.06			5
O1105	Victoria's lava lake (Vetreny Belt)		0.28	0.04			5
BV03	Komati (Barberton Greenstone Belt)		0.21	0.10	40.8[g]	50.6[g]	5
BV10	Komati (Barberton Greenstone Belt)		0.16	0.02	40.7[g]	50.3[g]	5
BV13	Komati (Barberton Greenstone Belt)		0.97	0.01	39.8[g]	46.8[g]	5
BV15	Komati (Barberton Greenstone Belt)		0.97	0.02	40.5[g]	48.7[g]	5
501-1	Weltevreden (Barberton Greenstone Belt)		0.35	0.01	45.3[g]	42.7[g]	3
Average komatiites			0.41	0.18			10

[a] 2se = 2 × standard deviation/√n.
[b] n = number of measurements.
[c] Day et al. (2010).
[d] Pringle et al. (2016).

[e] Helz et al. (1994).
[f] Puchtel et al. (2009).
[g] Puchtel et al. (2013).
[h] Peters and Day (2017).

to dryness, then re-dissolved in hydrochloric acid (6 N) and kept on the hotplate for 24 h at 120 °C. The Sr was purified using a two-step column chromatography technique in Teflon columns with 200 μL of Eichrom Sr-specific resin (20–50 μm) following the procedure described in Valdes et al. (2014). During the first step, the matrix is eluted with 3 N HNO_3 and subsequently the Sr is eluted with Milli-Q H_2O water. A second pass through the columns was considered essential to further purify Sr from the matrix. Purified Sr samples were then dried down and re-dissolved in 0.1 N HNO_3 for mass spectrometric analysis.

2.3. Mass spectrometry

Measurement of the stable Sr isotopic composition of samples were performed in medium resolution mode on a Thermo Fisher Neptune Plus MC-ICP-MS housed at the Institut de Physique du Globe de Paris. Ion beam intensities of ^{82}Kr, ^{83}Kr, ^{84}Sr, ^{85}Rb, ^{86}Sr, ^{87}Sr, ^{88}Sr were measured simultaneously using Faraday cups. A 100 ppb Sr solution was introduced into the mass-spectrometer using an Apex desolvating nebulizer, in conjunction with a jet sampler cone and H skimmer cone. A blank solution of 0.1 N HNO_3 was analyzed during each sequence and a blank correction was applied to each analysis. This approach is consistent with Woodhead et al. (2005), who suggested that performing on-peak-zeros prior to each analysis was the most effective method of dealing with Kr interference during MC-ICP-MS measurements. After subtracting the machine background the signal on the ^{82}Kr and ^{83}Kr was below 0.00001 V, and therefore there was no detectable Kr. Background measurements were below 1 mV on ^{88}Sr, which is insignificant relative to the signal of ^{88}Sr from the samples (> 5 V).

Instrumental mass bias was corrected using conventional standard–sample bracketing with the NIST SRM987 standard, a purified highly homogeneous Sr carbonate. Sr isotopic variations are reported in per mil as:

$$\delta^{88/86}\text{Sr}\ (‰) = \left[\frac{\left(\frac{^{88}\text{Sr}}{^{86}\text{Sr}}\right)_{sample}}{\left(\frac{^{88}\text{Sr}}{^{86}\text{Sr}}\right)_{SRM987}} - 1 \right] \times 1000 \quad (1)$$

Error is estimated from repeat measurements (~4 replicates) of the same solutions and is reported as twice the standard error (2se) where 2se = 2 × standard deviation/√n for n the number of measurements. The long-term reproducibility of the standard is ~30 ppm (2se). Three samples (SH25, RU0701 and EW9309-20D) were fully reprocessed two times (different dissolutions, chemistry and mass-spectrometer sessions) to test the reproducibility over time and to confirm the veracity of our chemical procedures. All duplicates have similar $\delta^{88/86}$Sr within 40 ppm and we use this conservative error for the meteoritic sample that we could only measure once due to mass constraints (Maralinga).

3. Results

Stable Sr isotopic compositions are presented in Tables 1 and 2 and in Fig. 1. The $\delta^{88/86}$Sr of OIB ranges from +0.16‰ to +0.46‰ with, an average of +0.29 ± 0.17‰ (n = 28, 2sd) (Table 1). MORB have a more restricted range between +0.27 and + 0.34‰, with an average of +0.31 ± 0.05‰ (n = 7, 2sd) (Table 1). Thesis results are consistent with previous data for basalts (Moynier et al., 2010; $\delta^{88/86}$Sr = +0.27 ± 0.05‰ n = 3; Charlier et al., 2012; $\delta^{88/86}$Sr = +0.30 ± 0.07‰ n = 8; Charlier et al. 2017 $\delta^{88/86}$Sr = +0.29 ± 0.05‰, n = 8). Kilauea Iki lava lake samples ($\delta^{88/86}$Sr = +0.31 ± 0.12‰; n = 10, 2sd), and komatiites ($\delta^{88/86}$Sr = +0.41 ± 0.18‰, n = 10, 2sd) have similar average values, within error (Table 1). Two Komati samples, BV13 and BV15, are highly enriched in the heavier isotopes of Sr $\delta^{88/86}$Sr = +0.97 ± 0.01‰ and $\delta^{88/86}$Sr = +0.97 ± 0.02 respectively), compared with the average value for others komatiites and terrestrial igneous rocks. When these are removed from the komatiite average, the $\delta^{88/86}$Sr value is similar to OIB and MORB samples, within error ($\delta^{88/86}$Sr = 0.29 ± 0.19‰, n = 8, 2sd).

Table 2
Stable strontium isotopic composition of chondrites relative to NIST SRM987.

Sample	Type	$\delta^{88/86}$Sr	2se[a]	n[b]	$\delta^{88/86}$Sr	2se[a]
Chondrites					Charlier et al. (2017)	
Vigarano	CV3	0.17	0.04	4	0.14	0.02
Felix	CO3	0.34	0.04	4	0.29	0.01
Isna	CO3	0.36	0.12	3		
Cold Bokkeveld	CM2	0.31	0.07	3	0.14	0.01
Jbilet Winselwan	CM2	0.34	0.11	5		
Maralinga	CK4	0.25		1		
Average CC		0.29	0.06	6		
Abee	EH4	0.36	0.03	4	0.43	0.01
Krymka	LL3.2	0.60	0.16	2		
Average chondrites		0.34	0.08	8		

[a] 2se = 2 × standard deviation/√n.
[b] n = number of measurements.

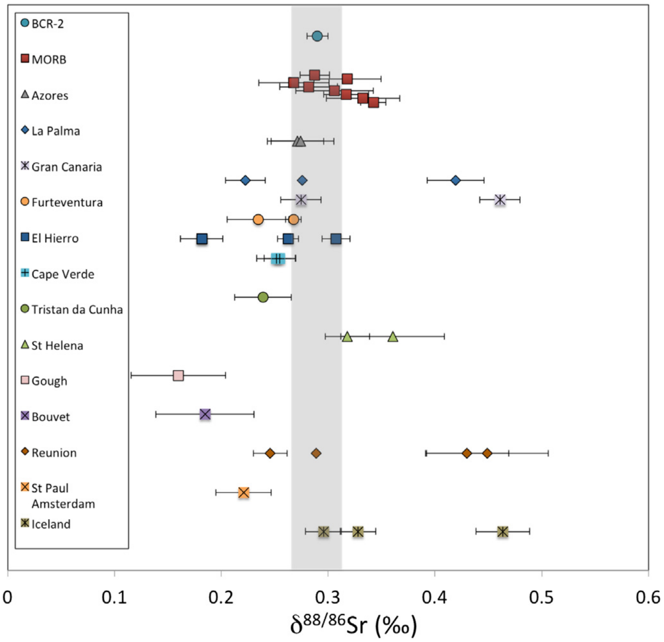

Fig. 1. $\delta^{88/86}$Sr for terrestrials basalts (MORB and OIB) and rock basaltic standard (BCR-2) highlighting the variation in OIB. The shaded area represents the average of basalts: $\delta^{88/86}$Sr = 0.29 ± 0.03‰.

The $\delta^{88/86}$Sr of chondrites vary from +0.17‰ to +0.60‰, with a mean of +0.34 ± 0.08‰. All chondrite samples that have been analyzed in both our laboratory by standard bracketing MC-ICP-MS, and by Charlier et al. (2017) at the Open University by double-spike TIMS have identical $\delta^{88/86}$Sr within error (Table 2) confirming the accuracy of the two different techniques. MC-ICPMS standard bracketing measurements are slightly less precise than double spike-TIMS measurements (~40 ppm here compared to ~20 ppm for TIMS, 2se in Charlier et al. 2017), however provide more sample throughput and the analysis of replicates. As such, this method was optimal for the current study, and subtle variations (under 40 ppm) are not considered in this study.

4. Discussion

4.1. Chondrite meteorites

The stable Sr isotopic compositions of most of the extra-terrestrial samples studied here have been previously measured and discussed (Moynier et al., 2010, Charlier et al., 2012, 2017). New measurements are presented here to directly compare with data collected during the same analytical campaign. We obtained the same $\delta^{88/86}$Sr values, within error, for Vigarano and Felix compared with Charlier et al. (2017). The two exceptions are the CM Cold Bokkeveld (+0.31 ± 0.07‰) which we found to be heavier than in the study by Charlier et al. (2017) (+0.14 ± 0.01‰), and the EH4 Abee which is slightly lighter (+0.36 ± 0.03‰) compared to the value obtained by Charlier et al., 2017 (+0.43 ± 0.01‰), but heavier than the value obtained by Moynier et al. (2010) (0.25 ± 0.09‰). The origin of these differences is not clear but could reflect localized low-temperature aqueous alteration on the CM pattern body, or simply heterogeneity in the sample. When we consider samples from the same meteoritic group, we find good agreement with the available literature data (Moynier et al., 2010, Charlier et al., 2012, 2017). As previously noted by Moynier et al. (2010), the $\delta^{88/86}$Sr of most chondrites cluster around ~ +0.3‰, with the exception of the CV (here, Vigarano with $\delta^{88/86}$Sr = +0.17 ± 0.04‰), which are lighter, due to the high abundance of isotopically light CAIs in CV compared to other chondrite groups.

4.2. Limited Sr isotopic fractionation during closed-system fractional crystallization

Kilauea Iki lava lake was formed during a single eruption and internal magmatic differentiation has led to a range of bulk chemical compositions through fractional crystallization processes. The MgO-rich samples (MgO > 7.5 wt%) are controlled by the removal or addition of olivine, while the most evolved samples (MgO < 7.5 wt%) are generated from a liquid from which experienced crystallization of augite, Fe-Ti oxides and plagioclase (Helz, 2012). Fractional crystallization and crystal settling have produced variations in the abundance of Sr, ranging from 291 to 506 ppm. In addition, Sr abundances are correlated with MgO contents of the samples, with the most evolved samples being the most Sr-rich (Fig. 2), due to the incompatibility of Sr in olivine. In contrast, $\delta^{88/86}$Sr shows limited variations and no correlation with MgO (Fig. 2; Fig. 4). Our results shows that fractional crystallization had limited effect on stable Sr isotopic compositions (< 0.1‰ for $\delta^{88/86}$Sr). This limited isotopic fractionation during differentiation is confirmed by the similar isotopic composition between ultramafic samples (komatiites) and basalts (Fig. 3). It is also confirmed by recent data on rhyolites ($\delta^{88/86}$Sr = +0.27 ± 0.15, 2sd, n = 33) that are isotopically similar to basalts (Charlier et al., 2017).

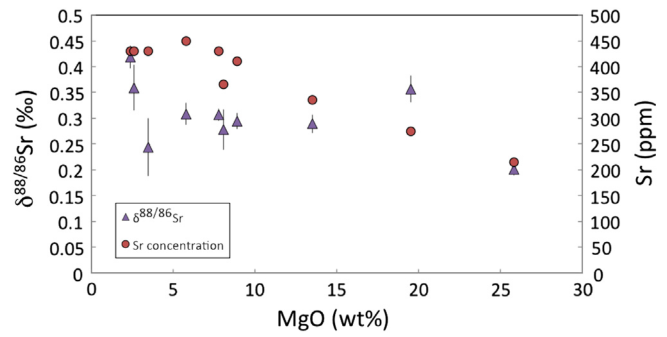

Fig. 2. Sr isotopic composition and Sr concentration of Kilauea Iki Lava lake samples relative to their MgO content.

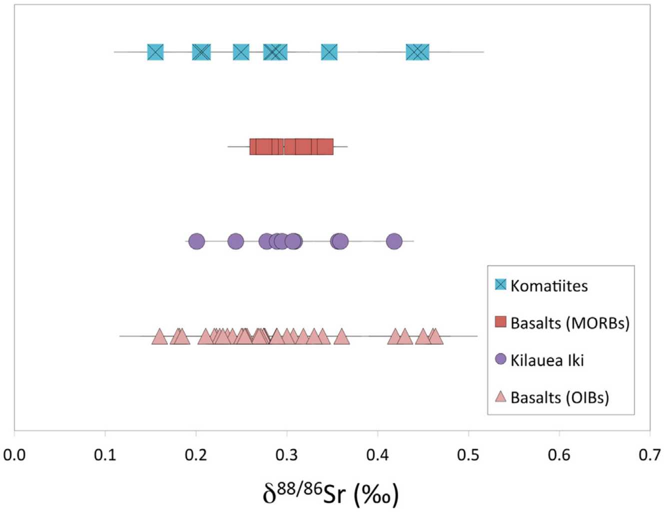

Fig. 3. Comparison of Sr isotopic composition of komatiites, MORB, OIB and Kilauea Iki lava lake samples.

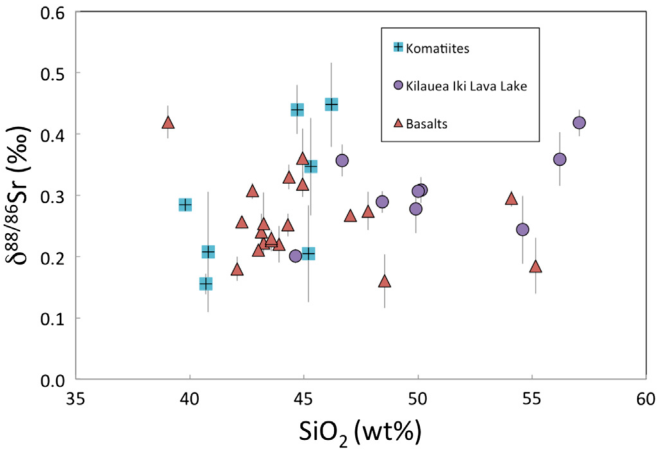

Fig. 4. Sr isotopic composition of OIB, Kilauea Iki lava lake samples and komatiites relative to their SiO_2 content (see Table 1 for published sources of SiO_2 data).

4.3. Variations of stable Sr isotopic composition in MORB and OIB samples

Collectively, MORB ($\delta^{88/86}$Sr = +0.31 ± 0.05‰, 2sd, n = 7) and OIB ($\delta^{88/86}$Sr = +0.29 ± 0.17‰, 2sd, n = 28) samples from the Atlantic, Pacific and Indian oceans are isotopically homogeneous, within uncertainties, and define an average value for basalts of +0.29 ± 0.16‰ (2sd, n = 35). In detail, the $\delta^{88/86}$Sr of OIB (from $\delta^{88/86}$Sr = +0.16 ± 0.04‰ to +0.46 ± 0.02‰) are more variable than for MORB (from $\delta^{88/86}$Sr = +0.27 ± 0.01‰ to +0.33 ± 0.03‰). Sr isotopic compositions of OIB from different localities are similar to first order. However, unlike MORB samples, some OIB exhibit small, but statistically significant, differences in isotopic composition. In particular, samples from Bouvet, Gough, St. Paul Amsterdam and two samples from El Hierro display enrichment in the lighter isotopes of Sr compared to the mean value of 0.29‰, and single samples from La Palma (LP03), Gran Canaria (GC0902), and Iceland (SK82-28), and two samples from La Reunion are enriched in the heavier Sr isotopes. Below, we consider possibilities that might explain these variations, which lie outside of analytical uncertainties.

4.3.1. Post-eruptive alteration processes

Compared to the other La Palma samples, LP03 is relatively enriched in the heavier Sr isotopes by ~0.2‰. Sample LP03 is an altered pillow lava (a picrite containing epigenetic clays, serpentine and calcite) with loss on ignition of > 6% and that was shown to have a radiogenic component that was removed after leaching (Day et al., 2010). The enrichment in the heavier isotopes could be due to post eruptive alteration, since Sr is strongly affected by silicate weathering. The $\delta^{88/86}$Sr value of many rivers draining volcanic terrains (including the Azores, La Reunion) are generally higher by 0.11‰ than average basalts (around 0.30‰) (Pearce et al. 2015). Pearce et al. (2015) showed that the heavy isotope enrichment of rivers could not be due to the weathering of isotopically heavier bedrocks as volcanic and plutonic rocks are known to have $\delta^{88/86}$Sr ~0.30‰. Instead, Pearce et al. (2015) proposed that weathering processes were responsible for the isotopic variations observed and suggested that the lighter Sr isotopes were concentrated into secondary phases that precipitated during alteration. They suggest this mechanism due to the negative correlation between $\delta^{88/86}$Sr and Sr/Na that highlights the removal of isotopically light Sr from the dissolved phase to the secondary phases that precipitate during weathering. Wei et al. (2013) measured stable and radiogenic Sr isotopic compositions of samples from the Xijiang river in South China and suggested that the high $\delta^{88/86}$Sr value in the river represents a contribution of silicate rock weathering. This implies an enrichment of the lighter isotopes for altered silicate rock, in agreement with Pearce et al. (2015). Furthermore, preferential incorporation of lighter isotopes is observed during carbonate precipitation (Böhm et al., 2012; Stevenson et al., 2014). These observations indicate that weathering processes could fractionate Sr isotopes between the bedrock and the drainage water and could lead to lighter isotopic compositions of Sr in altered rocks. However, while we observed light Sr isotopic compositions for the Gough, Bouvet and two samples from El Hierro, these samples do not show any evidence of weathering and require alternative explanations. BV2 comes from the 1955 eruption of Bouvet (O'Nions and Pankhurst, 1974) and ALR-40G has a LOI of 0.68% implying that theses samples were not altered. El Hierro samples have negative LOI suggesting that they are fresh, unaltered samples, consistent with their petrography (Day et al., 2010).

Seafloor alteration is a different process than sub-aerial weathering and the enrichment in the heavier isotopes for LP03 might be due to this process. The replacement of serpentine could lead to an enrichment in the heavier isotopes (see Sections 4.3.2), obscuring a possibly lighter isotopic composition due to the precipitation of calcite (e.g. Krabbenhöft et al., 2010; Böhm et al., 2012 and Vollstaedt et al., 2014).

To summarise, stable Sr isotopes suggest that weathering processes do not account for the light Sr isotope enrichment in OIB samples; however, seafloor alteration may explain the heavier Sr isotopic composition of samples LP03 and SK 82-28.

4.3.2. Recycled oceanic lithosphere

The variable oxygen and osmium isotopic compositions of samples from El Hierro and La Palma suggest a contribution of recycled oceanic crust and lithosphere during melting of pyroxenite-enriched peridotite lithologies (Day et al., 2009). Sedimentary materials usually have lighter Sr isotopic compositions ($\delta^{88/86}$Sr = 0.2‰, Krabbenhöft et al., 2010; Widanagamage et al., 2015; Stevenson et al., 2016) than typical oceanic crust represented by MORB (~0.30‰). Therefore, recycled sediments should either have a limited effect on the Sr isotopic composition, or slightly enrich them with the lighter isotopes, which is the opposite of what we observe for El Hierro and La Palma lavas. In contrast, altered oceanic crust should be enriched in the heavier isotopes of Sr. This is illustrated by the most hydrothermally altered samples (LP03), which is isotopically heavier than unaltered samples (see Section 4.3.1). Similarly, it has been found that serpentinite is itself enriched in the heavier isotopes of Sr (UB-N: $\delta^{88/86}$Sr = 0.54 ± 0.03‰; Ma et al., 2013). Therefore, contributions from altered oceanic crust could explain the heavier isotopic compositions measured for La Palma, Gran Canaria and La Reunion islands.

The same arguments can be made for Icelandic samples, which have been shown to have high ^{3}He/^{4}He ratios, negative Pb abundance anomalies and positive Nb, Ta and Sr abundance anomalies that are related to a recycled subducted lithosphere component in the plume (Breddam, 2002). To test the contribution of recycled material, we use a simple mass balance (to reach [Sr] = 100 ppm and $\delta^{88/86}$Sr = 0.4‰ for the heavy OIB samples) including a fraction of sedimentary material (1%; [Sr] = 200 ppm; $\delta^{88/86}$Sr = 0.02‰; Plank and Langmuir, 1998; Vollstaedt et al., 2014; Stevenson et al., 2016; Widanagamage et al., 2015), altered crust (46.5%; [Sr] = 160 ppm; $\delta^{88/86}$Sr = 0.43‰; Niu and Batiza, 1997), non-altered crust (50%; [Sr] = 120 ppm; $\delta^{88/86}$Sr = 0.29‰; Klein, 2003) and serpentinite (2.5%; [Sr] = 10 ppm; $\delta^{88/86}$Sr = 0.54‰; Alt et al., 2013; Ma et al., 2013) for the recycled fraction (in total: [Sr] = 140 ppm; $\delta^{88/86}$Sr = 0.50‰), and the contribution of the mantle ([Sr] = 20 ppm; $\delta^{88/86}$Sr = 0.29‰; this study; Palme and O'Neill, 2003) in generating the source of OIB. Using these values, we estimate that the fraction of recycled material must be approximately 53%, which is inconsistent with Pb, radiogenic Sr and trace elements constraints (Day et al., 2009). Hence, the contribution of recycled material is unlikely to be solely responsible for the enrichment in heavy isotopes observed for Gran Canaria, La Reunion islands and Iceland. Unfortunately, not enough Sr, Nd and Pb radiogenic isotopic composition data were available for the OIB samples studied here to assess the potential relationship with different recycled sources. More work will be needed to fully understand the origin of these outlier samples and to suggest an otherwise unidentified process that may be acting to generate these signatures.

4.4. The estimation of the stable Sr isotopic composition of the BSE

As discussed above, basaltic differentiation does not induce any measurable Sr isotopic fractionation, and with the exception of a few outliers, most basalts cluster within a very narrow range of Sr isotopic compositions, with an average of +0.28 ± 0.09‰ (2sd, n = 28). Furthermore, komatiites from three different regions ranging in age between 3.48 and 2.41 Ga have a similar average Sr isotopic composition ($\delta^{88/86}$Sr = 0.29 ± 0.19‰, 2sd, n = 8), excluding two outliers (BV13 and BV15), which is indistinguishable from the basalt average. The two outliers, BV13 and BV15 (from the upper part of Komati formation), were also found to be anomalous for Mo isotope composition (Greber et al., 2015). They are both enriched in the heavier isotopes of Mo by about 0.2‰/amu. The anomalous Sr (and Mo) isotopic compositions of BV13 and BV15 may have been inherited from mantle source heterogeneity or may have been the result of seafloor alteration and/or metamorphism that occur in the Komati lavas (Anhaeusser and Robb, 1980; Lowe, 1999). Since Sr isotopes are homogeneously distributed within a large set of basalts from around the world, as well as in the eight komatiites from four localities, we deem it as unlikely that the mantle source is isotopically heterogeneous for just these two komatiites. Instead, these two sample may have been affected by seafloor alteration or metamorphism. Greber et al. (2015) excluded an effect of alteration or metamorphism because of the correlation between $\delta^{98/95}$Mo and the MgO content and suggest a mantle source heterogeneity or a contribution of a more depleted mantle in theses komatiites. However, the Mo isotopic composition of the Barberton komatiites does not correlate with the Sr isotopic composition neither does the Sr isotopic composition with SiO_2 (Fig. 4), implying multiple processes acting on these samples. Previous studies have shown anomalies in oxygen isotopes (Byerly et al., 2017) and REE abundances (Puchtel et al., 2013) in olivine separates in the Barberton Greenstone Belt. Byerly et al. (2017) suggested that the light isotopic composition of O in these komatiites reflects heterogeneity of the Archean mantle, probably due to an unhomogenized residue from the magma ocean. Puchtel et al. (2013) suggested that the enrichment of incompatible elements in the olivine separates and the presence of inclusions of secondary minerals around the olivine grains are likely related to seafloor alteration or metamorphism. As discussed in Section 4.3.1, seafloor alteration could be the origin of the enrichment in heavy isotopes of Sr in these komatiites, while metamorphism is a process that has not been effectively studied for Sr stable isotopes. Experimental studies on bulk rocks have demonstrated that during heating the Sr isotopic composition of the bulk rocks are unaffected (e.g. Baadsgaard and Van Breemen, 1970). Metamorphism is known to homogenize Sr isotopes in a rock that remains in a closed system. It is therefore unlikely that metamorphism is the origin of the isotopic fractionation of the two Barbeton komatiites, and we prefer alteration as the cause for the enrichment of Sr heavy isotopes.

Since komatiites are produced by high degrees of partial melting (e.g. Herzberg, 1992), they should have quantitatively extracted Sr from their source and represent the best estimate for the composition of the mantle. The similarity of Sr isotopic compositions between komatiite, OIB and MORB samples as well as the limited Sr isotopic variability between the Kilauea Iki samples represent strong evidence for limited isotopic fractionation during igneous processes. Their average Sr isotopic composition can be used to estimate the stable Sr isotopic composition of the mantle to be $+0.29 \pm 0.16$‰ ($n = 46$, 2sd). When the average of OIB, MORB and komatiites (excluding the two outliers) are taken separately, the $\delta^{88/86}$Sr of the BSE can be estimated to be $+0.30 \pm 0.02$‰ (2sd) which is in agreement with previous work (Moynier et al., 2010: $\delta^{88/86}$Sr = 0.27‰ and Charlier et al., 2012: $\delta^{88/86}$Sr = 0.29 ± 0.07‰). Since the continental crust contains about 10% of the Earth's Sr (using a simple mass balance calculation), it should also be considered in the evaluation of the Sr isotopic composition of the bulk silicate Earth (BSE). However, the absence of Sr isotopic fractionation between komatiites, basalts and granites ($\delta^{88/86}$Sr = 0.31 ± 0.09‰ and $\delta^{88/86}$Sr = 0.28 ± 0.03‰, Moynier et al., 2010) and the limited isotopic fractionation within the Kilauea Iki Lava lake rock series suggests that crustal material should have a similar stable Sr isotopic composition to the present-day mantle.

The high concentration of Sr in carbonates (up to 2000 ppm, Plank and Langmuir, 1998) and their enrichment in Sr lighter isotopes (~0.3‰) could alter the stable Sr isotopic composition of the BSE. However, since carbonates represent only 0.01% of the weight of the crust (Wedepohl, 1995) they should not significantly affect the stable Sr isotopic composition of the BSE. Indeed, using the estimation of the Sr concentration of the continental and oceanic crust (Wedepohl, 1995; Hofmann, 1988) and an average of Sr concentration in carbonate (Plank and Langmuir, 1998), basalt and granite, the Sr budget of carbonates is roughly calculated to be ~6% for the continental crust and ~3% in the oceanic crust. Therefore, it can be inferred that the present estimate of the mantle composition is similar to the composition of the bulk silicate Earth. This assumption can be tested in the future by analyzing the Sr isotopic composition of shales. Furthermore, since Sr is a lithophile element, the Earth's core is nominally Sr free, and the Sr isotopic composition of the BSE can then be considered as the bulk Earth composition. Finally, the fact that the 2.4 Ga, 2.7 Ga, 3.27 Ga and 3.48 Ga old komatiites all have similar Sr isotopic compositions ($\delta^{88/86}$Sr = 0.27 ± 0.03, 0.36 ± 0.11, 0.18 ± 0.05, and 0.28 ± 0.06‰, respectively) with modern basalts, suggests that the composition of Earth's mantle has not changed over at least the past 3.48 Ga.

5. Conclusions

In this study, we measured the Sr isotopic composition of a wide range of OIB, MORB, and komatiites from different localities and of different ages. The similarity of the $\delta^{88/86}$Sr between all of the samples implies little fractionation effects during and after the formation of the basaltic and komatiitic magmas. Komatiites show a range of Sr isotopic compositions similar to that of all the basalts studied, enabling the estimation of the Sr isotopic composition for the BSE to be $+0.30 \pm 0.02$‰ (2sd), in agreement with previous work (Moynier et al., 2010 and Charlier et al., 2012). The Sr isotopic composition of carbonaceous chondrites is similar to terrestrial composition, except for a CV chondrite sample that is enriched in refractory inclusions and thus subsequently enriched in the light isotopes.

Acknowledgments

We thank two anonymous reviewers, and the Editor, Klaus Mezger, for their constructive comments. FM acknowledges funding from the European Research Council under the H2020 framework program/ERC grant agreement #637503 (Pristine) and financial support of the UnivEarthS Labex program at Sorbonne Paris Cité (ANR-10-LABX-0023 and ANR-11-IDEX-0005-02), and the ANR through a chaire d'excellence Sorbonne Paris Cité. We also thank the IPGP multidisciplinary program PARI, and by Paris-IdF region SESAME Grant No. 12015908. Finally, we are grateful to Brandon Mahan for proof- reading the manuscript.

References

Albarède, F., Tamagnan, V., 1988. Modelling the recent geochemical evolution of the Piton de la Fournaise Volcano, Reunion Island, 1931–1986. J. Pet. 29, 997–1030.

Alt, J.C., Schwarzenbach, E.M., Früh-Green, G.L., Shanks III, W.C., Bernasconi, S.M., Garrido, C.J., Crispini, L., Gaggero, L., Padrón-Navarta, J.A., Marchesi, C., 2013. The role of serpentinites in cycling of carbon and sulfur: seafloor serpentinization and subduction metamorphism. Lithos 178, 40–54.

Anhaeusser, C.R., Robb, L.J., 1980. Regional and detailed field and geochemical studies of Archaean trondhjemitic gneisses, migmatites and greenstone xenoliths in the southern part of the Barberton Mountain Land, South Africa. Precambrian Res. 11 (3–4), 373–397.

Baadsgaard, H., Van Breemen, O., 1970. Thermally-induced migration of Rb and Sr in adamellite. Eclogae Geol. Helv. 63, 31–44.

Badullovich, N., Moynier, F., Creech, J., Teng, F.-Z., Sossi, P.A., 2017. Tin isotopic fractionation during igneous differentiation and Earth's mantle composition. Geochem. Persp. Let. 5, 24–28.

Birck, J.-L., Allègre, C.J., 1973. ^{87}Rb-^{87}Sr systematics of Muntsche Undra Mafic Pluton (Kola Peninsula, USSR). Earth Planet. Sci. Lett. 20, 266–274.

Böhm, F., Eisenhauer, A., Tang, J., Dietzel, M., Krabbenhöft, A., Kisakürek, B., Horn, C., 2012. Strontium isotope fractionation of planktic foraminifera and inorganic calcite. Geochim. Cosmochim. Acta 93, 300–314.

Breddam, K., 2002. Kistufell: primitive melt from the Iceland mantle plume. J. Pet. 43, 345–373.

Breddam, K., Kurz, M.D., Storey, M., 2000. Mapping out the conduit of the Iceland mantle plume with helium isotopes. Earth Planet. Sci. Lett. 176, 45–55.

Byerly, B.L., Kareem, K., Bao, H., Byerly, G.R., 2017. Early earth mantle heterogeneity revealed by light oxygen isotopes of Archaean komatiites. Nature Geosc. 10, 871–875.

Charlier, B.L.A., Nowell, G.M., Parkinson, L.J., Kelley, S.P., Pearson, D.G., Burton, K.W., 2012. High temperature strontium stable isotope behaviour in the early solar system and planetary bodies. Earth Planet. Sci. Lett. 329-330, 31–40.

Charlier, B.L.A., Parkinson, I.J., Burton, K.W., Grady, M.M., Wilson, C.J.N., Smith, E.G.C., 2017. Stable strontium isotopic heterogeneity in the solar system from double-spike data. Geochim. Persp. Let. 4, 35–40.

Chen, H., Savage, P.S., Teng, F.-Z., Helz, R.T., Moynier, F., 2013. Zinc isotope fractionation during magmatic differentiation and the isotopic composition of the bulk earth. Earth Planet. Sci. Lett. 369-370, 34–42.

Claude-Ivanaj, C., Joron, J.L., Allègre, C.J., 2001. ^{238}U-^{230}Th-^{226}Ra fractionation in historical lavas from the Azores: long-lived source heterogeneity vs. metasomatism fingerprints. Chem. Geol. 176, 295–310.

Day, J.M.D., Hilton, D.R., 2011. Origin of ^{3}He/^{4}He ratios in HIMU-type basalts constrained from Canary Island lavas. Earth Planet. Sci. Lett. 305, 226–234.

Day, J.M.D., Pearson, D.G., Macpherson, C.G., Lowry, D., Carracedo, J.C., 2009. Pyroxenite-rich mantle formed by recycled oceanic lithosphere: oxygen–osmium isotope evidence from Canary Island lavas. Geology 37, 555–558.

Day, J.M.D., Pearson, D.G., Macpherson, C.G., Lowry, D., Carracedo, J.C., 2010. Evidence for distinct proportions of subducted oceanic crust and lithosphere in HIMU-type mantle beneath El Hierro and La Palma, Canary Islands. Geochim. Cosmochim. Acta 74, 6565–6589.

De Souza, G.F., Reynolds, B.C., Kiczka, M., Bourdon, B., 2010. Evidence for mass-dependent isotopic fractionation of strontium in a glaciated granitic watershed. Geochim. Cosmochim. Acta 75, 2596–2614.

Fietzke, J., Eisenhauer, A., 2006. Determination of temperature-dependent stable strontium (^{88}Sr/^{86}Sr) fractionation via bracketing standard MC-ICP-MS. Geochem. Geophys. Geosys. 7, 8.

Garapić, G., Jackson, M.G., Hauri, E.H., Hart, S.R., Farley, K.A., Blusztajn, J.S., Woodhead, J.D., 2015. A radiogenic isotopic (He–Sr–Nd–Pb–Os) study of lavas from the Pitcairn hotspot: implications for the origin of EM-1 (enriched mantle 1). Lithos 228–229, 1–11.

Geist, D.J., Fornari, D.J., Kurz, M.D., Harpp, K.S., Adam Soule, S., Perfit, M.R., Koleszar, A.M., 2006. Submarine Fernandina: magmatism at the leading edge of the Galapagos hot spot. Geochem. Geophys. Geosyst. 7, Q12007.

Graham, D.W., Humpris, S.E., Jenkins, W.J., Kurz, M.D., 1992. Helium isotope geochemistry of some volcanic rocks from Saint Helena. Earth Planet. Sci. Lett. 110, 121–131.

Greber, N.D., Puchtel, I.S., Nägler, T.F., Mezger, K., 2015. Komatiites constrain molybdenum isotope composition of the Earth's mantle. Earth Planet. Sci. Lett. 421, 129–138.

Halicz, L., Segal, I., Fruchter, N., Stein, M., Lazar, B., 2008. Strontium stable isotopes fractionate in the soil environments? Earth Planet. Sci. Lett. 272, 406–411.

Hanyu, T., Kaneoka, I., 1997. The uniform and low 3He/4He ratios of HIMU basalts as evidence for their origin as recycled materials. Nature 390, 273–276.

Hart, S.R., Jackson, M.G., 2014. Ta'u and Ofu/Olosega volcanoes: the 'twin Sisters' of Samoa, their P, T, X melting regime, and global implications. Geochem. Geophys. Geosyst. 15, 2301–2318.

Helz, R.T., 2012. Trace element analyses of core samples from the 1967-1988 drillings of Kilauea Iki Lava Lake, Hawaii. US Geological Survey Open File Report 2012–1050, 1–56.

Helz, R.T., Thornber, C.R., 1987. Geothermometry of Kilauea Iki lava lake, Hawaii. Bull. Volcanol. 49, 651–668.

Helz, R.T., Kirschenbaum, H., Marinenko, J.W., Qian, R., 1994. Whole rock analyses of core samples from the 1967, 1975, 1979 and 1981 drillings of Kilauea Iki lava lake, Hawaii. US Geological Survey Open File Report 94–684, 1–65.

Herzberg, C., 1992. Depth and degree of melting of komatiites. J. Geophys. Res. 97, 4521–4540.

Hofmann, A.W., 1988. Chemical differentiation of the earth: the relationship between mantle, continental crust and oceanic crust. Earth Planet. Sci. Lett. 90, 297–314.

Jackson, M.G., Hart, S.R., Koppers, A.A.P., Staudigel, H., Konter, J., Blusztajn, J., Kurz, M., Russell, J.A., 2007a. The return of subducted continental crust in Samoan lavas. Nature 448, 684–687.

Jackson, M.G., Kurz, M.D., Hart, S.R., Workman, R.K., 2007b. New Samoan lavas from Ofu Island reveal a hemispherically heterogeneous high 3He/4He mantle. Earth Planet. Sci. Lett. 264, 360–374.

Kato, C., Moynier, F., Foriel, J., Teng, F.-Z., Puchtel, I.S., 2017. The gallium isotopic composition of the bulk silicate earth. Chem. Geol. 448, 164–172.

Kawabata, H., Hanyu, T., Chang, Q., Kimura, J.-I., Nichols, A.R.L., Tatsumi, Y., 2011. The petrology and geochemistry of St. Helena alkali basalts: evaluation of the oceanic crust-recycling model for HIMU OIB. J. Pet. 52, 791–838.

Klein, 2003. Geochemistry of the igneous oceanic crust. Treatise on Geochemistry 3, 433–463.

Krabbenhöft, A., Eisenhauer, A., Böhm, F., Vollstaedt, H., Fietzke, J., Liebetrau, V., Augustin, N., Peucker-Ehrenbrink, B., Müller, M.N., Horn, C., Hansen, B.T., Nolte, N., Wallmann, K., 2010. Constraining the marine strontium budget with natural strontium isotope fractionations (^{87}Sr/^{86}Sr, $\delta^{88/86}$Sr) of carbonates, hydrothermal solutions and river waters. Geochim. Cosmochim. Acta 75, 4097–4109.

Kurz, M.D., Curtice, J., Fornari, D., Geist, D., Moreira, M., 2009. Primitive neon from the center of the Galapagos hotspot. Earth Planet. Sci. Lett. 286, 23–34.

LeRoex, A.P., 1985. Geochemistry, mineralogy and magmatic evolution of the basaltic and trachytic lavas from Gough Island, South Atlantic. J. Pet. 26, 149–186.

Lodders, K., 2003. Solar system abundances and condensation temperatures of the elements. Astrophys. J. 591, 1220–1247.

Lowe, D.R., 1999. Geologic evolution of the Barberton Green-stone Belt and vicinity. In: Geological Evolution of the Barberton Greenstone Belt. 329. Geological Society of America, pp. 287–312.

Ma, J., Wei, G., Liu, Y., Ren, Z.Y., Xu, Y., Yang, Y., 2013. Precise measurement of stable ($\delta^{88/86}$Sr) and radiogenic (^{87}Sr/^{86}Sr) strontium isotope ratios in geological standard reference materials using MC-ICP-MS. Chin. Sci. Bull. 58, 3111–3118.

Millet, M.-A., Doucelance, R., Schiano, P., David, K., Bosq, C., 2008. Mantle plume heterogeneity versus shallow-level interactions: a case study, the São Nicolau Island, Cape Verde archipelago. J. Volcanol. Geotherm. Res. 176, 265–276.

Moreira, M., Staudacher, T., Sarda, P., Schilling, J.-G., Allègre, C.J., 1995. A primitive plume neon component in MORB: the Shona ridge-anomaly, South Atlantic (51–52°S). Earth Planet. Sci. Lett. 133, 367–377.

Moreira, M., Breddam, K., Curtice, J., Kurz, M.D., 2001. Solar neon in the Icelandic mantle: new evidence for an undegassed lower mantle. Earth Planet. Sci. Lett. 185, 15–23.

Moynier, F., Agranier, A., Hezel, D.C., Bouvier, A., 2010. Sr stable isotope composition of earth, the moon, Mars, Vesta and meteorites. Earth Planet. Sci. Lett. 300, 359–365.

Nebel, O., Mezger, K., Westrenen, W., 2011. Rubidium isotopes in primitive chondrites: constraints on Earth's volatile element depletion and lead isotope evolution. Earth Planet. Sci. Lett. 305, 309–316.

Niu, Y., Batiza, R., 1997. Trace element evidence from seamounts for recycled oceanic crust in the Eastern Pacific mantle. Earth Planet. Sci. Lett. 148, 471–483.

Ohno, T., Hirata, T., 2007. Simultaneous determination of mass-dependent isotopic fractionation and radiogenic isotope variation of strontium in geochemical samples by multiple collector-ICP-mass spectrometry. Anal. Sci. 23, 1275–1280.

O'Nions, R.K., Pankhurst, R.J., 1974. Petrogenetic significance of isotope and trace element variations in volcanic rocks from the mid-Atlantic. J. Pet. 15, 603–634.

Palme, O'Neill, 2003. Cosmochemical estimates of mantle composition. Treatise on Geochemistry 2, 1–38.

Papanastassiou, D.A., Wasserburg, G.J., 1969. Initial strontium isotopic abundances and the resolution of small time differences in the formation of planetary objects. Earth Planet. Sci. Lett. 5, 361–376.

Parkinson, I.J., Burton, K.W., Mokadem, F., Charlier, B.L., 2007. High-precision double Sr isotope measurements: applications to geochemistry and cosmochemistry. American Geophy. Union 88, 52 Abstract.

Patchett, P.J., 1980. Sr isotopic fractionation in Ca-Al inclusions from the Allende meteorite. Nature 283, 438–441.

Pearce, C.R., Parkinson, I., Gaillardet, J., Charlier, B.L.A., Mokadem, F., Burton, K.W., 2015. Reassessing the stable (of $\delta^{88/86}$Sr) and radiogenic (^{87}Sr/^{86}Sr) strontium isotopic composition of marine inputs. Geochim. Cosmochim. Acta 157, 125–146.

Peters, B.J., Day, J.M.D., 2017. A geochemical link between plume head and tail volcanism. Geochem. Persp. Let. 5, 29–34.

Plank, T., Langmuir, C.H., 1998. The chemical composition of subducting sediment and its consequences for the crust and the mantle. Chem. Geol. 145, 325–394.

Pringle, E.A., Moynier, F., Savage, P.S., Jackson, M.G., Moreira, M., Day, J.M.D., 2016. Silicon isotopes reveal recycles altered oceanic crust in the mantle sources of Ocean Island basalts. Geochim. Cosmochim. Acta 189, 282–295.

Puchtel, I.S., Walker, R.J., Brandon, A.D., Nisbet, E.G., 2009. Pt-Re-Os and Sm-Nd isotope and HSE and REE systematics of the 2.7 Belingwe and Abiti komatiites. Geochim. Cosmochim. Acta 73, 6367–6389.

Puchtel, I.S., Blichert-Toft, J., Touboul, M., Walker, R.J., Byerly, G.R., Nisbet, E.G., Anhaeusser, C.R., 2013. Insight into early earth from Barbeton komatiites: evidence from lithophile isotope and trace element systematics. Geochim. Cosmochim. Acta 108, 63–90.

Puchtel, I.S., Walker, R.J., Touboul, M., Nisbet, E.G., Byerly, G.R., 2014. Insights into early earth from the Pt–Re–Os isotope and highly siderophile element abundance systematics of Barberton komatiites. Geochim. Cosmochim. Acta 125 (C), 394–413.

Puchtel, I.S., Touboul, M., Blichert-Toft, J., Walker, R.J., Brandon, A.D., Nicklas, R.W., Kulikov, V.S., Samsonov, A.V., 2016. Lithophile and siderophile element systematics of Earth's mantle at the Archean-Proterozoic boundary: evidence from 2.4 Ga komatiites. Geochim. Cosmochim. Acta 180, 227–255.

Raddatz, J., Liebetrau, V., Rüggeberg, A., Hathorne, E., Krabbenhöft, A., Eisenhauer, A., Böhm, F., Vollstaedt, H., Fietzke, J., López Correa, M., Freiwald, A., Dullo, W.-Chr, 2013. Stable Sr-isotopes, Sr/Ca, Mg/Ca and Mg/Li ratios in the scleractinian cold-water coral *Lophelia pertusa*. Chem. Geol. 352, 143–152.

Rickers, F., Fichtner, A., Trampert, J., 2013. The Iceland–Jan Mayen plume system and its impact on mantle dynamics in the North Atlantic region: evidence from full-waveform inversion. Earth Planet. Sci. Lett. 367, 39–51.

Savage, P.S., Moynier, F., Chen, H., Shofner, G., Siebert, J., Badro, J., Puchtel, I.S., 2015. Copper isotope evidence for large-scale sulphide fractionation during Earth's differenciation. Geochem. Persp. Let. 1, 53–64.

Shalev, N., Segal, I., Lazar, B., Gavrieli, I., Fietzke, J., Eisenhauer, A., Halicz, L., 2013. Precise determination of $\delta^{88/86}$Sr in natural samples by double-spike MC-ICP-MS and its TIMS verification. J. Analyt. Atomic Spectrometry(6).

Stevenson, E.I., Hermoso, M., Rickaby, R.E.M., Tyler, J.J., Minoletti, F., Parkinson, I.J., Mokadem, F., Burton, K.W., 2014. Controls on stable strontium isotope fractionation in coccolithophores with implications for the marine Sr cycle. Geochim. Cosmochim. Acta 128, 225–235.

Stevenson, E.I., Aciego, S.M., Chutcharavan, P., Parkinson, I.J., Burton, K.W., Blakowski, M.A., Arendt, C.A., 2016. Insight into combined radiogenic and stable strontium isotopes as tracers for weathering processes in subglacial environments. Chem. Geol. 429, 33–43.

Teng, F.-Z., Wadhwa, M., Helz, R.T., 2007. Investigation of magnesium isotope fractionation during basalt differentiation: implications for a chondritic composition of the terrestrial mantle. Earth Planet. Sci. Lett. 261, 84–92.

Teng, F.-Z., Dauphas, N., Helz, R.T., 2008. Iron isotope fractionation during magmatic differentiation in Kilauea Iki Lava Lake. Science 320, 1620–1622.

Teng, F.-Z., Li, W.-E., Ke, S., Marty, B., Dauphas, N., Huang, S., Wu, F.-Y., Pourmand, A., 2010. Magnesium isotope composition of the earth and chondrites. Geochim. Cosmochim. Acta 75, 4150–4166.

Teng, F.-Z., Dauphas, N., Helz, R.T., Gao, S., Huang, S., 2011. Diffusion-driver magnesium and iron isotope fractionation in Hawaiian olivine. Earth Planet. Sci. Lett. 308, 317–324.

Teng, F.Z., Dauphas, N., Watkins, J.M., 2017. Non-traditional Stable Isotopes: Retrospective and Prospective. In: Teng, F.Z., Dauphas, N., Watkins, J.M. (Eds.), Non-traditional Stable Isotopes. Rev. Mineral. Geochem., pp. 82.

Tomascak, P.B., Tera, F., Jelz, R.T., Walker, R.J., 1999. The absence of lithium isotope fractionation during basalt differentiation: new measurements by multicollector sector ICP-MS. Geochim. Cosmochim. Acta 63, 907–910.

Valdes, M.C., Moreira, M., Foriel, J., Moynier, F., 2014. The nature of Earth's building blocks as revealed by calcium isotopes. Earth Planet. Sci. Lett. 394, 135–145.

Vollstaedt, H., Eisanhauer, A., Wallmann, K., Böhm, F., Fietzke, J., Liebetrau, V., Krabbenhöft, Farkaš, J., Tomašovych, A., Raddatz, J., Veizer, J., 2014. The Phanerozoic $\delta^{88/86}$Sr record of seawater: new constraints on past changes in oceanic carbonate fluxes. Geochim. Cosmoschim. Acta 128, 249–265.

Wedepohl, K.H., 1995. The composition of the continental crust. Geochim. Cosmochim. Acta 59 (7), 1217–1232.

Wei, G., Ma, J., Liu, Y., Xie, L., Lu, W., Dend, W., Ren, Z., Zeng, T., Yang, Y., 2013. Seasonal changes in the radiogenic and stable strontium isotopic composition of Xijang River water: implications for chemical weathering. Chem. Geol. 343, 67–75.

Widanagamage, I.H., Griffith, E.M., Singer, D.M., Scher, H.D., Buckley, W.P., Senko, J.M., 2015. Controls on stable Sr-isotope fractionation in continental barite. Chem. Geol. 411, 215–227.

Woodhead, J., Swearer, S., Hergt, J., Maas, R., 2005. In situ Sr-isotope analysis of carbonates by LA-MC-ICP-MS: interference corrections, high spatial resolution and an example from otolith studies. J. Anal. At. Spectrom. 20, 22–27.

Workman, R.K., Hart, S.R., Jackson, M., Regelous, M., Farley, K.A., Blusztajn, J., Kurz, M., Staudigel, H., 2004. Recycled metasomatized lithosphere as the origin of the enriched mantle II (EM2) end- member: evidence from the Samoan volcanic chain. Geochem. Geophys. Geosyst. 5, Q04008.

Wright, T.L., 1973. Magma mixing as illustrated by the 1959 eruption, Kilauea volcano, Hawaii. Geol. Soc. Am. Bull. 84, 849–858.